

**IMPACT OF CARBONACEOUS AEROSOLS ON THE  
REGIONAL CLIMATE OF INDIA USING A  
REGIONAL CLIMATE MODEL**

**SUDIPTA GHOSH**



**CENTRE FOR ATMOSPHERIC SCIENCES  
INDIAN INSTITUTE OF TECHNOLOGY DELHI  
OCTOBER 2022**



© **Indian Institute of Technology Delhi (IITD), New Delhi, 2022**



**IMPACT OF CARBONACEOUS AEROSOLS ON THE  
REGIONAL CLIMATE OF INDIA USING A  
REGIONAL CLIMATE MODEL**

*by*

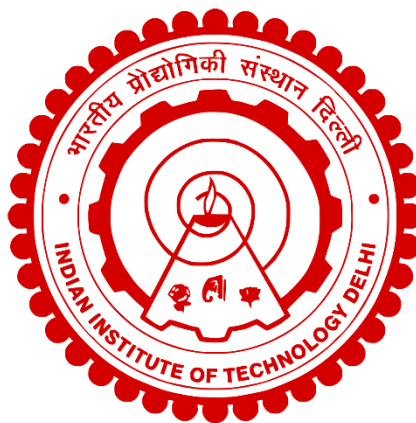
**SUDIPTA GHOSH**

**Centre for Atmospheric Sciences**

*Submitted*

**in fulfilment of the requirements of the degree of Doctor of Philosophy**

*to the*



**INDIAN INSTITUTE OF TECHNOLOGY DELHI**

**OCTOBER 2022**



*Dedicated*

*To*

*Maa and Baba*



## Certificate

This is to certify that the thesis entitled “**Impact of carbonaceous aerosols on the regional climate of India using a regional climate model**” being submitted by **Ms Sudipta Ghosh** for the award of the degree of **Doctor of Philosophy**, is a record of the original bonafide research work carried out by her. She has worked under my guidance and supervision and has fulfilled the requirements for the submission of this thesis. The results presented in this thesis have not been submitted in part or full to any University or Institution for the award of any degree/diploma.

Prof Sagnik Dey

Professor

Centre for Atmospheric Sciences,

Indian Institute of Technology Delhi,

Hauz Khas, New Delhi-110016, India



## Acknowledgements

Words fall short when it comes to acknowledging the people who were there during my PhD journey. Still, to begin with, I would like to express my deepest gratitude and sincere thanks to my PhD supervisor Dr Sagnik Dey. This endeavour would not have been possible without his constant support, encouragement and immense knowledge insights. He not only extended his academic advice but also motivated me to explore new challenges and further push my limits. His positive approach and occasional reality checks make challenging targets doable. He provided me with all possible facilities and opportunities to nurture my research skills. His ideologies helped me evolve as a better person on both professional and personal fronts.

I want to acknowledge all the professors, the Head of the Centre for Atmospheric Sciences and respectable CRC members for their valuable suggestions and scientific feedback during all the semester progress reports. They facilitated me with a great learning and research environment. Besides, I would like to thank Dr Dilip Ganguly for sharing his knowledge and insights on climate modelling. I also thank Dr S.K. Dash for helping me collaborate with the RegCM4 core development team in Trieste, Italy. I thank my SRC members for guiding my academic journey with their expertise.

I want to thank IIT Delhi CAS storage facilities and IIT Delhi HPC, PADUM, for providing a hassle-free computation facility. I sincerely thank DST Inspire Fellowship for funding my entire PhD research. I also extend my gratitude to USIEF Fulbright-Kalam Fellowship for funding my 9-months Fulbright Foreign Student Program in the USA. Sincere thanks to ICTP, Italy, for supporting a 3-month research visit at ICTP.

I am fortunate to be hosted by Dr Nicole Riemer from the Department of Atmospheric Sciences, University of Illinois, Urbana-Champaign (UIUC), Illinois, USA, during my

Fulbright Foreign Student Program. Her constant support, insightful ideas and feedback throughout my Fulbright journey and beyond is a true blessing for my thesis work and research career. I thank UIUC's high-performance computer, Keeling, for facilitating computation and storage facilities.

I am also blessed to work with the founder of RegCM, Dr Filippo Giorgi and current chief development scientist, Graziano Giuliani from Earth System Physics at The Abdus Salam Institute of Theoretical Physics (ICTP), Trieste, Italy. Their expertise helped me to learn and use RegCM4 with more scientific confidence.

My PhD tenure is blessed with people who are more than peers and friends. I am deeply indebted to Dr Sourangsu Chowdhury, who guided me since my master's. His support and motivation paved the way for CAS and Dr Dey's research group. Big thanks to Dr Parul Srivastava, Namita Sinha, Dr Tanuja Nigam and Dr Thumree Sarkar for being there through all ups and downs. I want to thank Sofiya, Soumi, Rohit, Sushovan and other labmates for making my stay at CAS a memorable journey. Sincere thanks to my seniors Dr Sushant Das, Dr Pushpraj Tiwari, Dr Abhisekh Upadhyay, for all the scientific discussions and helpful tips on handling model errors. My journey at CAS is incomplete without thanking Mr Vijay Kumar for all his logistic support and administrative insights. I also want to thank Shashank Sharma for always being there to share a cup of coffee at the Amul.

Life at IIT Delhi is not complete without my hostel, Himadri. I want to thank the hostel warden, caretaker and all the staff for making my stay comfortable. In addition, five lovely human beings made my hostel room a home away from home. Dr Sukanya Ghosh is a friend, philosopher and guide. I want to thank her and Anushruti Vagrani for handling all the mood swings and late-night tears. I want to thank Dr Srishti Srivastava for making WB-04 worth

returning to and Dr Rabab Anjum for all the biryani and positive outlook. I also want to thank Saroj Bijarnia for being there during the evening walks.

I want to thank Puja Roy, Preetha Sarkar, Arka Mitra, Shruti Sankolli, Sujan Pal, Lina Rivelli Zea and Prateek Sharma for making my Fulbright stay memorable. Special thanks to Ms Soma Dey Ghosh Mam and Ms Maitrayee Bera Mam for helping, arranging and providing all the necessities required to settle in a new country.

My PhD journey has blessed me with two beautiful and kind souls – Dr Esha Baidya Kayal and Dr Dalim Kumar Baidya. My deepest gratitude for all the love, affection and support they continue to bestow on me and have made Delhi my second hometown. I also want to thank Dr Thilaka Muthiah, Dr Sulagna Bhattacharjee and Dr Souvik Maitra for their constant love and support.

No words or phrases can pen down my indebt towards my family members for their constant love and support. Ma, Baba, Bhaibhai, Atanu Da and Anagh are my greatest pillar of strength. While Ma and Baba taught me to walk strong and motivated, Bhaibhai and Atanu Da gave me the wings to fly by taking all responsibilities back at home. I am blessed and thankful to my in-laws, who always encouraged and supported my research career. Last but not least, special thanks to my husband, Mr Rounick Dutta, who stands rock-solid in all my academic endeavours.

In the end, I want to thank the almighty God for blessing me with patience, perseverance, strength and determination to complete this journey.

Date: 31.10.2022

Sudipta Ghosh



## Abstract

According to the latest IPCC report, eastern and south Asia, particularly India and China, continue to significantly contribute to the global aerosol burden. India is the home to the second-largest population in the world. Therefore, climate change and air pollution have significant socio-economic consequences, especially in an emerging economy like India. Short-lived climate pollutants (SLCPs) are a class of aerosols that act as both climate forcers and air pollutants. SLCPs exist in the atmosphere from a few hours to a few days or months, and carbonaceous aerosols (CAs) are an essential category of SLCPs. CAs are mainly produced either directly (as primary particles) or indirectly (as secondary particles due to chemical reactions in the atmosphere) due to incomplete combustion of fossil fuels and open-air biomass burning. CA constitutes black carbon (BC) and organic carbon (OC). BC exerts a positive forcing while OC exerts a negative forcing at the top of the atmosphere. Therefore, mitigating emissions of CAs are expected to result in crucial climate-health co-benefits.

Despite their major role in climate forcing, considerable knowledge gaps exist in this region regarding their life cycles and radiative feedback. These gaps arise due to complex topography, heterogeneous aerosol distribution, measurements at limited locations, and disagreement of the inter-model estimates. Knowledge gained from field studies is limited to point locations, and the meteorological response to the CA radiative forcing cannot be investigated using observations. The magnitude of dynamic response can be estimated by climate models. Accurate representation of CAs in the climate models is critical for reducing uncertainty in estimated climate forcing. Model uncertainties can result from the model's inability to accurately represent aerosol processes, composition and emission fluxes.

This thesis investigates the direct radiative effects of CAs on the Indian climate using a regional climate model - RegCM4.6. To achieve the thesis objective, at first two of the above-

mentioned model uncertainties – (i) ageing (aerosol process) of the carbonaceous aerosols in a regional climate model RegCM4.6 and (ii) emission inventory have been addressed. The model is simulated over the South-Asian CORDEX domain for 2010 only for the two-step augmentation. Then the augmented RegCM4.6 has been simulated with total and source-apportioned anthropogenic aerosols to study the CA direct radiative effects for the period 2006-2015. All the numerical experiments conducted in this thesis considered anthropogenic aerosols only.

First, a dynamic ageing parameterization scheme has been implemented in RegCM4.6. Freshly emitted CAs are hydrophobic in nature. Conversion of hydrophobic to hydrophilic carbonaceous aerosol is called ‘ageing’ and, in general, is influenced by physical processes like condensation and coagulation. In RegCM4.6, an e-folding fixed ageing time of 1.15 days (~27.6 hours) is considered, while in reality, the ageing is dynamic and depends on coagulation and condensation. After implementing the dynamic ageing scheme, it is found that the conversion of hydrophobic to hydrophilic aerosols took place in <10 hours over the polluted regions, especially over the Indo-Gangetic Basin (IGB), with almost 6-7% increment in anthropogenic AOD (AAOD). The results demonstrate the importance of improving aerosol representation in the climate models for a more realistic climate impact assessment. Furthermore, this work is the first-ever study on aerosol ‘ageing’ conducted in the Indian context.

The dynamic ageing scheme represented a more realistic atmosphere, but the underestimation in CA mass concentrations persisted. In the next step, a region-specific emission inventory has been incorporated in the model. Simulations have been carried out to understand the relative importance of aerosol processes and emission fluxes and their combined impact in improving the model performance. Results demonstrated that the combined effect of the new ageing scheme and regional emissions reduced the model-to-observation mismatch to

a greater extent than the improvement due to only either of them. Therefore, the effect of each of the model uncertainty is non-linear, and the mean normalised bias for BC concentration reduced from -69% to -51% w.r.t the in-situ data, with the highest improvement observed in the polluted IGB where the regional background aerosol loading is high. The customization enhanced AAOD from 6-7% (improvement due to only ageing) to ~19% (due to ageing and regional emissions together). The results suggest that the combined effect of emission fluxes and more realistic aerosol processes are crucial to improving the aerosol representation in the climate models.

After customizing RegCM4.6, direct radiative effects of anthropogenic aerosols have been investigated. Considering only CA aerosols are far from the realistic atmosphere, total anthropogenic direct radiative effects have been considered. However, only CA simulations have been performed to separate out the sulphate contribution. The results show that the augmented model is able to capture the seasonal CA distribution even on a longer timescale. Additionally, the anthropogenic feedback mechanism on the Indian climate is not uniform from 2006-2015 and varies seasonally. Tracer concentrations are highest during winter and lowest during the monsoon. AAOD showed higher values over more polluted IGB, resulting in a strong surface dimming. This, in turn, lowered the monsoon rainfall over the IGB. Variations in wind convergence, transported anthropogenic aerosols and higher(lower) residence time due to lower(higher) removal of the tracers resulted in positive (negative)  $\Delta$ AAOD. The current study is the first of its kind where the CA direct radiative forcing has been analysed simultaneously for all four seasons.

The CA direct radiative forcing is source-specific over Asia. Therefore, in the final working chapter of the thesis, anthropogenic direct radiative effects have been investigated for five major anthropogenic sources. For this, the ‘subtraction’ method is followed, where in each successive simulation, emissions from one particular sector have been switched off, and the

changes in radiative forcing and meteorological response relative to the simulations in the previous chapter (control for this case) are interpreted as the contribution of that particular sector. The domestic sector emerged as the dominant contributor to BC and OC over the IGB, while the industries and the energy sector are the dominant contributors to sulphate (Sadavarte & Venkataraman, 2014). In fact, domestic sector emerged to be the most significant contributor to atmospheric heating (almost 40 – 50%) throughout the year and over the entire country. Other sectors contributed an annual average of, within, 30% to the atmospheric heating with varying seasonal magnitudes.

The current thesis work demonstrates the importance of addressing model uncertainties for an improved model-to-observation ratio. Also, long-term, seasonal and source-apportioned analysis is crucial for investigating aerosol direct radiative forcing under changing climate.

## सारांश

नवीनतम आईपीसीसी रिपोर्ट के अनुसार, पूर्वी और दक्षिण एशिया, विशेष रूप से भारत और चीन, वैश्विक एयरोसोल बोझ में महत्वपूर्ण योगदान दे रहे हैं। भारत दुनिया में दूसरी सबसे बड़ी आबादी का घर है। इसलिए, जलवायु परिवर्तन और वायु प्रदूषण के महत्वपूर्ण सामाजिक-आर्थिक परिणाम हैं, खासकर भारत जैसी उभरती अर्थव्यवस्था में। अल्पकालिक जलवायु प्रदूषक (SLCP) एरोसोल का एक वर्ग है जो जलवायु प्रेरक बल और वायु प्रदूषक दोनों के रूप में कार्य करता है। एसएलसीपी कुछ घंटों से लेकर कुछ दिनों या महीनों तक वातावरण में मौजूद रहते हैं, और कार्बोनेसियस एरोसोल (CA) एसएलसीपी की एक महत्वपूर्ण श्रेणी है। सी ए मुख्य रूप से या तो प्रत्यक्ष रूप से (प्राथमिक कणों के रूप में) या अप्रत्यक्ष रूप से (वायुमंडल में रासायनिक प्रतिक्रियाओं के कारण द्वितीयक कणों के रूप में) जीवाश्म ईंधन के अधूरे दहन और खुली हवा में बायोमास जलने के कारण उत्पन्न होते हैं। सीए, ब्लैक कार्बन (BC) और ऑर्गेनिक कार्बन (OC) से गठित है। बी सी एक सकारात्मक बल लगाता है जबकि ओ सी वायुमंडल के शीर्ष पर एक नकारात्मक बल लगाता है। इसलिए, सी ए के उत्सर्जन को कम करने से महत्वपूर्ण जलवायु-स्वास्थ्य सह-लाभ होने की उम्मीद है।

जलवायु बल में उनकी प्रमुख भूमिका के बावजूद, इस क्षेत्र में उनके जीवन चक्र और विकिरण प्रतिक्रिया के संबंध में काफी ज्ञान अंतराल मौजूद है। ये अंतराल जटिल स्थलाकृति, विषम एरोसोल वितरण, सीमित स्थानों पर माप और अंतर-मॉडल अनुमानों की असहमति के कारण उत्पन्न होते हैं। क्षेत्र अध्ययनों से प्राप्त ज्ञान बिंदु स्थानों तक सीमित है, और सीए विकिरण बल के लिए मौसम संबंधी प्रतिक्रिया की टिप्पणियों का उपयोग करके जांच नहीं की जा सकती है। इस गतिशील प्रतिक्रिया की भयावहता का अनुमान जलवायु मॉडल द्वारा लगाया जा सकता है। जलवायु मॉडल में सीए का सटीक प्रतिनिधित्व अनुमानित जलवायु बल में अनिश्चितता को कम करने के लिए महत्वपूर्ण है। एरोसोल प्रक्रियाओं संयोजन और

उत्सर्जन फ्लक्स का सटीक रूप से प्रतिनिधित्व करने में मॉडल की अक्षमता के परिणामस्वरूप मॉडल की अनिश्चितता हो सकती है। ।

यह थीसिस एक क्षेत्रीय जलवायु मॉडल - रेग सी एम 4.6 का उपयोग करके भारतीय जलवायु पर सीए के प्रत्यक्ष विकिरण प्रभावों की जांच करती है। थीसिस उद्देश्य को प्राप्त करने के लिए, उपर्युक्त मॉडल अनिश्चितताओं में से पहले दो - (i) कार्बोनेसियस एरोसोल की उम्र बढ़ने (एयरोसोल प्रक्रिया) और (ii) उत्सर्जन सूची को - रेग सी एम 4.6 मॉडल में संबोधित (पता) किया गया है। मॉडल को केवल दो-चरणीय वृद्धि के लिए 2010 के लिए दक्षिण-एशियाई कॉर्डेक्स डोमेन पर सिम्युलेटेड किया गया है। फिर संवर्धित रेग सी एम 4.6 को 2006-2015 की अवधि के लिए CA प्रत्यक्ष विकिरण प्रभावों का अध्ययन करने के लिए कुल और स्रोत-विभाजित मानवजनित एरोसोल के साथ सिम्युलेटेड किया गया है। इस थीसिस में किए गए सभी संख्यात्मक प्रयोगों को केवल मानवजनित एरोसोल माना जाता है।

सबसे पहले, एक गतिशील उम्र बढ़ने के मानकीकरण योजना को रेग सी एम 4.6 में लागू किया गया है। ताजा उत्सर्जित सी ए प्रकृति में हाइड्रोफोबिक हैं। हाइड्रोफोबिक एरोसोल का हाइड्रोफिलिक कार्बोनेसियस एरोसोल में रूपांतरण ही 'उम्र बढ़ने की प्रक्रिया' कहा जाता है और यह सामान्य तौर पर, संक्षेपण और जमावट जैसी भौतिक प्रक्रियाओं से प्रभावित होता है। रेग सी एम 4.6 में, 1.15 दिनों (~ 27.6 घंटे) का एक ई-फोल्डिंग निश्चित उम्र बढ़ने का समय माना जाता है, जबकि वास्तव में, उम्र बढ़ने की प्रक्रिया गतिशील है और जमावट और संक्षेपण पर निर्भर करती है। गतिशील उम्र बढ़ने की प्रक्रिया की योजना को लागू करने के बाद, यह पाया गया है कि हाइड्रोफोबिक का हाइड्रोफिलिक एरोसोल में रूपांतरण <10 घंटे में प्रदूषित क्षेत्रों में हुआ, विशेष रूप से इंडो-गंगा बेसिन (आई जी बी) पर, मानवजनित एओडी (एएओडी) में लगभग 6-7% की वृद्धि के साथ। अधिक यथार्थवादी परिणाम, जलवायु प्रभाव मूल्यांकन के लिए जलवायु मॉडल में एरोसोल प्रतिनिधित्व में सुधार के महत्व को प्रदर्शित करते हैं। इसके

अलावा, यह काम भारतीय संदर्भ में एयरोसोल 'एजिंग, उम्र बढ़ने की प्रक्रिया' पर किया गया पहला अध्ययन है।

गतिशील उम्र बढ़ने की योजना ने अधिक यथार्थवादी वातावरण का प्रतिनिधित्व किया, लेकिन सीए द्रव्यमान परिमाण वास्तविक से कम आंका गया। अगले चरण में, मॉडल में एक क्षेत्र-विशिष्ट उत्सर्जन सूची शामिल की गई है। एरोसोल प्रक्रियाओं और उत्सर्जन प्रवाह के सापेक्ष महत्व और मॉडल के प्रदर्शन को बेहतर बनाने में उनके संयुक्त प्रभाव को समझने के लिए सिमुलेशन किए गए हैं। परिणामों ने प्रदर्शित किया कि नई उम्र बढ़ने की प्रक्रिया की योजना और क्षेत्रीय उत्सर्जन के संयुक्त प्रभाव ने मॉडल-से-अवलोकन (ऑब्ज़र्वेशन) के बेमेल को केवल उनमें से किसी एक के कारण सुधार की तुलना में काफी हद तक कम कर दिया। इसलिए, प्रत्येक मॉडल अनिश्चितता का प्रभाव गैर-रैखिक (नॉन लीनियर) है, और बीसी परिमाण के लिए सामान्यीकृत पूर्वाग्रह त्रुटि -69% से घटकर -51% हो गया है, इन-सीटू डेटा के साथ, प्रदूषित आईजीबी में उच्चतम सुधार देखा गया है जहां क्षेत्रीय पृष्ठभूमि एरोसोल लोडिंग अधिक है। अनुकूलन ने एएओडी को 6-7% (केवल उम्र बढ़ने के कारण सुधार) से ~ 19% (उम्र बढ़ने और क्षेत्रीय उत्सर्जन के कारण सुधार) तक बढ़ाया। परिणाम बताते हैं कि जलवायु मॉडल में एरोसोल प्रतिनिधित्व में सुधार के लिए उत्सर्जन प्रवाह और अधिक यथार्थवादी एरोसोल प्रक्रियाओं का संयुक्त प्रभाव महत्वपूर्ण है।

रेग सी एम 4.6 को अनुकूलित करने के बाद, मानवजनित एरोसोल के प्रत्यक्ष विकिरण प्रभावों की जांच की गई है। केवल सीए एयरोसोल को ध्यान में रखते हुए किया गया सिमुलेशन यथार्थवादी वातावरण से अलग है, इसलिए कुल मानवजनित प्रत्यक्ष विकिरण प्रभावों पर विचार किया गया है। हालांकि, सल्फेट योगदान को अलग करने के लिए केवल सीए सिमुलेशन का प्रदर्शन किया गया है। परिणाम दिखाते हैं कि संवर्धित मॉडल लंबे समय के पैमाने पर भी मौसमी सीए वितरण को पकड़ने (सिमुलेट करने) में सक्षम है। इसके अतिरिक्त, भारतीय जलवायु पर मानवजनित प्रतिक्रिया तंत्र 2006-2015 से एक समान नहीं है और

मौसमी रूप से बदलता रहता है। ट्रेसर परिमाण सर्दियों के दौरान सबसे अधिक और मानसून के दौरान सबसे कम होता है। एएओडी ने अधिक प्रदूषित आईजीबी की तुलना में उच्च मान दिखाया, जिसके परिणामस्वरूप एक मजबूत सरफेस डिमिंग मिला। इसने बदले में, आईजीबी पर अधिक मानसूनी वर्षा को कम कर दिया। पवन अभिसरण में बदलाव, परिवहन किए गए मानवजनित एरोसोल और कम (उच्च) ट्रेसर को हटाने के परिणामस्वरूप जनित उच्च (निचले) निवास समय (रेजिडेंस टाइम) के कारण सकारात्मक (नकारात्मक)  $\Delta$  एएओडी प्राप्त हुआ। वर्तमान अध्ययन अपनी तरह का पहला है जहां सभी चार मौसमों के लिए सीए प्रत्यक्ष विकिरण बल का एक साथ विश्लेषण किया गया है।

इस, थीसिस के अंतिम कार्य अध्याय में, पांच प्रमुख मानवजनित स्रोतों के लिए मानवजनित प्रत्यक्ष विकिरण प्रभावों की जांच की गई है। इसके लिए, 'घटाव' पद्धति का पालन किया जाता है, जहां प्रत्येक क्रमिक अनुकरण में, एक विशेष क्षेत्र से उत्सर्जन को बंद कर दिया गया है, और पिछले अध्याय में सिमुलेशन के सापेक्ष विकिरण बल और मौसम संबंधी प्रतिक्रिया में परिवर्तन (इस मामले के लिए नियंत्रण) उस विशेष क्षेत्र के योगदान के रूप में व्याख्या की जाती है। घरेलू क्षेत्र आईजीबी पर बीसी और ओसी के प्रमुख योगदानकर्ता के रूप में उभरा, जबकि उद्योग और ऊर्जा क्षेत्र सल्फेट के प्रमुख योगदानकर्ता हैं (सदावर्ते और वेंकटरमन, 2014) ) वास्तव में, घरेलू क्षेत्र पूरे वर्ष और पूरे देश में वायुमंडलीय तापन (लगभग 40 - 50%) में सबसे महत्वपूर्ण योगदानकर्ता के रूप में उभरा। अन्य क्षेत्रों ने अलग-अलग मौसमी परिमाण के साथ वायुमंडलीय तापन में वार्षिक औसत का योगदान 30% के भीतर किया।

वर्तमान थीसिस कार्य एक बेहतर मॉडल-से-अवलोकन अनुपात के लिए मॉडल अनिश्चितताओं को संबोधित करने के महत्व को दर्शाता है। इसके अलावा, बदलती जलवायु के तहत एरोसोल प्रत्यक्ष विकिरण बल की जांच के लिए दीर्घकालिक, मौसमी और स्रोत-विभाजित विश्लेषण महत्वपूर्ण है।

# Table of Contents

**Certificate**

**Acknowledgements**

**Abstract**

**Contents**

**List of Abbreviations**

**List of Figures**

<b>Chapter 1: Introduction and literature review .....</b>	<b>1</b>
1.1 Introduction .....	2
1.1.1 Earth's climate and radiation budget .....	3
1.1.2 Atmospheric aerosols .....	6
1.1.3 Aerosol radiative effect .....	6
1.2 Literature review .....	9
1.2.1 Observational-based studies .....	15
1.2.2 Model-based studies .....	17
1.3 Research gaps.....	20
1.4 Objectives of the thesis .....	22
1.5 Organisation of the thesis.....	22

**Chapter 2: Implementation of a dynamic ageing parameterisation scheme in a regional climate model, RegCM4 .....24**

2.1 Introduction .....25

2.2 RegCM4 .....25

    2.2.1 Model description .....25

    2.2.2 Physical Parameterisation Schemes.....28

    2.2.3 Aerosol Module .....30

    2.2.4 Aerosol-Radiation Interaction .....32

    2.2.5 Model Execution.....33

2.3 Implementation of carbonaceous aerosol ageing parameterisation scheme in RegCM4.6 .....34

2.4 Global emission inventory .....35

2.5 Experiment design and data used .....37

2.6 Impact of dynamic ageing on the spatiotemporal distribution of carbonaceous aerosols .....40

2.7 Impact of dynamic ageing on aerosol optical properties.....49

2.8 Impact of dynamic ageing on aerosol radiative forcing .....53

2.9 Summary .....57

**Chapter 3: Customization of the RegCM4 to the choice of emission inventories over the Indian subcontinent .....60**

3.1 Introduction .....61

3.2 Regional emission inventory .....62

3.3 Experiment design.....	63
3.4 Validation data used .....	65
3.4.1 TRMM precipitation data .....	65
3.4.2 In-situ BC data.....	65
3.4.3 MERRA-2 data .....	66
3.4.4 MISR aerosol data .....	66
3.5 Simulation of meteorology by the augmented model .....	67
3.6 Spatiotemporal distribution of simulated carbonaceous aerosols by the augmented model .....	69
3.6.1 Spatial distribution of anthropogenic aerosols .....	69
3.6.2 Vertical distribution of carbonaceous aerosols.....	78
3.7 Simulation of aerosol optical properties by the augmented model .....	82
3.8 Simulation of aerosol radiative forcing by the augmented model .....	84
3.9 Summary .....	87
<b>Chapter 4: Climate feedback of carbonaceous aerosols over India using a augmented RegCM4 .....</b>	<b>89</b>
4.1 Introduction .....	90
4.2 Experiment design and data used .....	91
4.3 Emission data .....	91
4.4 Meteorological data for validation .....	92
4.5 Experiment design.....	93

4.6 Spatiotemporal distribution of anthropogenic aerosols simulated by the augmented model .....	94
4.7 Climatological distribution of aerosol optical properties simulated by the augmented model.....	101
4.8 Simulation of meteorological fields due to the aerosol-radiation direct interactions ..	107
4.8.1 Validation of simulated meteorological fields.....	107
4.8.2 Dynamic response due to aerosol-radiative feedback .....	110
4.9 Summary .....	121
<b>Chapter 5: Relative contributions of major emitting sectors to the climate forcing of carbonaceous aerosols.....</b>	<b>123</b>
5.1 Introduction .....	124
5.2 Experiment design and data used .....	125
5.3 Emission data .....	125
5.4 Meteorological data.....	128
5.5 Experiment design.....	128
5.6 Spatio-temporal distribution of anthropogenic aerosol in absence of each major sector .....	129
5.7 Simulation of aerosol optical properties and direct radiative forcing in absence of each major sector.....	135
5.7.1 Variation of anthropogenic AOD .....	136
5.7.2 Variation of aerosol radiative forcing.....	137
5.8 Summary .....	140

<b>Chapter 6: Conclusions and Future prospects.....</b>	<b>142</b>
6.1 Major limitations .....	143
6.2 Conclusions .....	143
6.3 Future Prospects .....	147
<b>References.....</b>	<b>147</b>
<b>Appendix</b>	



## List of Abbreviations

Aerosol optical depth ( <b>AOD</b> )	Integrated Campaign on Aerosol and Radiation Budget ( <b>ICARB</b> )
Aerosol Radiative Forcing over India Network ( <b>ARFINET</b> )	Intergovernmental Panel on Climate Change ( <b>IPCC</b> )
Agricultural waste burning ( <b>AWB</b> )	Intertropical convergence zone ( <b>ITCZ</b> )
Anthropogenic aerosol optical depth ( <b>AAOD</b> )	January-February ( <b>JF</b> )
Biosphere-Atmosphere Transfer Scheme ( <b>BATS</b> )	June-July-August-September ( <b>JJAS</b> )
Black carbon ( <b>BC</b> )	Latent heat ( <b>LH</b> )
Brown carbon ( <b>BrC</b> )	March-April-May ( <b>MAM</b> )
Carbonaceous aerosols ( <b>CA</b> )	Mean normalised bias ( <b>MNB</b> )
Climate Research Unit ( <b>CRU</b> )	Model for Ozone and Related chemical Tracers ( <b>MOZART</b> )
Cloud condensation number ( <b>CCN</b> )	Modern-Era Retrospective Analysis for Research and Applications, version 2 ( <b>MERRA-2</b> )
Confidence Interval ( <b>CI</b> )	Multiangle Imaging Spectroradiometer ( <b>MISR</b> )
Coordinated Regional Climate Downscaling Experiment ( <b>CORDEX</b> )	National Center for Atmospheric Research ( <b>NCAR</b> )
Consortium for Small-Scale Modelling in Climate Mode ( <b>COSMO-CLM</b> )	NCAR Community Climate Model Version 3 ( <b>CCM3</b> )
Domestic ( <b>DOM</b> )	NCAR Mesoscale Model Version 5 ( <b>MM5</b> )
Elevated heat pump ( <b>EHP</b> )	October-November-December ( <b>OND</b> )
Energy ( <b>ENE</b> )	Organic carbon ( <b>OC</b> )
Global climate model ( <b>GCM</b> )	Ozone Monitoring Instrument ( <b>OMI</b> )
Greenhouse gases ( <b>GHG</b> )	Particulate matter ( <b>PM</b> )
Hydrophilic BC ( <b>BC_HL</b> )	Peninsular India ( <b>PI</b> )
Hydrophilic OC ( <b>OC_HL</b> )	Providing Regional Climates for Impacts Studies ( <b>PRECIS</b> )
Hydrophobic BC ( <b>BC_HB</b> )	Regional climate models ( <b>RCM</b> )
Hydrophobic OC ( <b>OC_HB</b> )	Regional Climate Model version 4.6 ( <b>RegCM4.6</b> )
Indian Meteorological Department ( <b>IMD</b> )	
Indian Ocean Experiment ( <b>INDOEX</b> )	
Indo-Gangetic Basin ( <b>IGB</b> )	
Industries ( <b>IND</b> )	
Infra-red ( <b>IR</b> )	

Sensible heat (**SH**)

Short-lived climate pollutants (**SLCP**)

Shortwave radiative forcing (**SWRF**)

Sub-grid Explicit Moisture Scheme  
(**SUBEX**)

Top of the atmosphere (**TOA**)

Transport (**TRA**)

Tropical Rainfall Measuring Mission  
(**TRMM**)

Ultraviolet (**UV**)

Weather Research Forecasting  
(**WRF**)

## List of Figures

Figure 1.1: Schematic representation of the factors influencing Earth’s climate and energy budget. Figure adapted from the graphical abstract of IPCC AR6, Chapter 7 (Forster et al., 2021). .....	3
Figure 1.2: Schematic representation of the global mean energy budget with clouds (top panel) and without clouds (bottom panel). The figure has been adapted from (Wild et al., 2015, 2019) .....	5
Figure 1.3: Global mean effective radiative forcing of various climate forcings from 1750-2019. The figure has been adapted from the IPCC AR6 report (Forster et al., 2021). .....	7
Figure 1.4: Schematic representation of aerosol interacting with the earth’s radiation. The figure has been adapted from IPCC AR4 (Forster et al., 2007.).....	8
Figure 1.5: Optical and molecular classification of carbonaceous aerosols (Pöschl, 2003)...	10
Figure 1.6: Climatology of black carbon extinction coefficient at 550 nm from MERRA-2 reanalysis data for the period 2006-2015.....	14
Figure 2.1: Annual emission ( $\text{kg/m}^2/\text{s}$ ) of BC, OC and $\text{SO}_2$ for 2010 over the study region. .	36
Figure 2.2: Seasonal variation of ageing timescale anomaly (in hours) of carbonaceous aerosols at 1000 hPa w.r.t the fixed ageing timescale of 27.6 hours [1.15 day]. The upper level of the colour scale bar has been capped at 140 h (i.e., the ageing time scale is $(27.6+140)$ h = 167.6 h or 7 days), and the lower limit has been capped at -20 h (i.e., the ageing time scale is $(27.6 - 20)$ h = 7.6 h). The figure shows the total domain of the simulation, and the area within the black rectangle represents the study domain. ....	36

Figure 2.3: Seasonal variation of column-averaged ageing time-scale anomaly (in hours) of carbonaceous aerosols from 925-700 hPa w.r.t fixed ageing time-scale of 27.6 hours [1.15 day]. The upper level of the scale bar has been capped at 140 hrs (i.e. $27.6 + 140 = 167.6$ hrs, almost 7 days), and the lower limit has been capped at -20 hrs (i.e. $27.6 - 20 = 7.6$ hrs). ....	39
Figure 2.4: Spatial distribution of mean BC columnar burden ( $\text{mg}/\text{m}^2$ ) with fixed ageing [a and b] and mean BC surface mass concentration ( $\mu\text{g}/\text{m}^3$ ) [c and d], corresponding changes due to the new ageing scheme [(e,f) for columnar burden and (g, h) for surface mass concentration] respectively for JF and JJAS 2010. Dotted lines represent a 75% significance level for burden and an 85% significance level for mass concentration. ....	42
Figure 2.5: Removal processes for BC ( $\text{mg}/\text{m}^2/\text{day}$ ): Dry deposition flux difference between Expt_dyn and Expt_fix at 90% significant level for both the seasons (a, b, c and d) and wet deposition flux difference values between Expt_dyn and Expt_fix at 90% significant level for JF and 80% significant level for JJAS (e, f, g and h).....	43
Figure 2.6: Changes in the columnar burden ( $\text{mg}/\text{m}^2$ ) of BC_HB (top panel) and BC_HL (2nd panel) and the surface mass concentration ( $\mu\text{g}/\text{m}^3$ ) of BC_HB (3rd panel) and BC_HL (bottom panel) for two contrasting seasons due to the change in ageing parameterisation scheme. ....	46
Figure 2.7: Spatial distribution of mean OC columnar burden ( $\text{mg}/\text{m}^2$ ) with fixed ageing [a and b] and mean OC surface mass concentration ( $\mu\text{g}/\text{m}^3$ ) [c and d], corresponding changes induced due to new ageing scheme [(e,f) for columnar burden and (g, h) for surface mass concentration] respectively for JF and JJAS 2010. Dotted lines represent a 75% significance level for burden and an 85% significance level for mass concentration. ....	48

Figure 2.8: Removal processes for OC ( $\text{mg}/\text{m}^2/\text{day}$ ): Dry deposition flux difference between Expt_dyn and Expt_fix at 90% significant level for both the seasons (top panel) and wet deposition flux difference values between Expt_dyn and Expt_fix at 90% significance for JF and at 80% significant level for JJAS (bottom panel). .....	49
Figure 2.9: Spatial distribution of % difference of anthropogenic AOD (a and b) and precipitation difference between Expt_dyn and Expt_fix (c and d) for two contrasting seasons. ....	50
Figure 2.10: Spatial distributions of BC hydrophobic to the hydrophilic ratio (top panel) and OC hydrophobic to the hydrophilic ratio (bottom panel) for two contrasting seasons.....	53
Figure 2.11: Mean surface shortwave radiative forcing ( $\text{W}/\text{m}^2$ ) in Expt_dyn and corresponding changes w.r.t Expt_fix for winter (a, d) and monsoon (g, j), mean TOA aerosol shortwave forcing ( $\text{W}/\text{m}^2$ ) in Expt_dyn and corresponding changes w.r.t Expt_fix for winter (b, e) and monsoon (h, k) and mean atmospheric heating ( $\text{W}/\text{m}^2$ ) in Expt_dyn and related changes w.r.t Expt_fix for winter (c, f) and monsoon (i, l). Dotted contours represent an 85% significance level.....	54
Figure 2.12: Spatial patterns of seasonal net downward shortwave flux during (a, b, c and d) JF and (e, f, g, h) JJAS in (a, b, e, f) all-sky and (c, d, g, h) clear-sky conditions from (a, c, e, g) CERES and (b, d, f, h) model. ....	55
Figure 2.13: Evaluation between model-derived surface downward shortwave flux and CERES surface shortwave flux ( $\text{W}/\text{m}^2$ ) for winter (JF).....	56
Figure 2.14 : Evaluation between model-derived surface downward shortwave flux and CERES surface shortwave flux ( $\text{W}/\text{m}^2$ ) for monsoon (JJAS).....	56

Figure 3.1: Seasonal variation of the global and regional emission inventories in kg/m <sup>2</sup> /s for BC (1st and 2nd rows), OC (3rd and 4th rows) and SO <sub>2</sub> (5th and 6th rows). .....	63
Table 2: Detailed description of the experiments .....	64
Figure 3.2: Comparison of the augmented model simulated seasonal temperature distribution (°C) with CRU temperature data. ....	68
Figure 3.3: Spatial distribution of monsoon precipitation (mm/day) bias for the monsoon season (JJAS) w.r.t TRMM data (j).....	68
Figure 3.4: Spatial distribution of surface mass concentration (µg/m <sup>3</sup> ) of BC (a, b) and OC (d, e) in 2010 over the Indian subcontinent using (left) the default and (middle) the augmented model configurations. Figures 3.4.c and 3.4.f represent the corresponding percentage differences due to the augmented model set-up (positive values imply an increase in mass concentration). The vertical distributions (shown in Figures 3.10, 3.11 and 3.12) are analysed for the IGP and PI sub-regions marked by boxes in the panels of the left column. ....	70
Figure 3.5: Spatial patterns of mean seasonal surface BC concentration (µg/m <sup>3</sup> ) over India (1st column) using the default set-up and percentage differences in the (2nd and 3rd columns) modified and (4th column) augmented configurations relative to the default set-up.....	71
Figure 3.6: Locations of the 24 cities where BC concentrations were measured during the study period and used to evaluate the augmented model performance. The colour of the circles indicates the percentage increase in BC concentrations due to the implementation of the dynamic scheme. The circles' size indicates the percentage increase in BC concentrations due to the combined impact of the ageing scheme and regional inventory in the augmented model. ....	72

Figure 3.7: Comparison of mean annual simulated BC surface concentration ( $\mu\text{g}/\text{m}^3$ ) using the default and augmented model with in-situ measurements from 24 cities across India. Locations of the cities are shown in Figure 3.6. RMSE (in $\mu\text{g}/\text{m}^3$ ) and $R^2$ between the augmented model simulations and surface measurements are also provided. ....	74
Figure 3.8: Comparison of spatial patterns of annual (top panel) BC and (bottom panel) OC column burden ( $\text{mg}/\text{m}^2$ ). ....	75
Figure 3.9: Top panel - MERRA-2 BC burden ( $\text{mg}/\text{m}^2$ ). Middle and bottom panels - Percentage difference of BC columnar burden simulated by the model w.r.t MERRA-2 BC burden ( $\text{mg}/\text{m}^2$ ). ....	77
Figure 3.10: Top panel - MERRA-2 OC burden ( $\text{mg}/\text{m}^2$ ). Middle and bottom panels - Percentage difference of OC columnar burden simulated by the model w.r.t MERRA-2 OC burden ( $\text{mg}/\text{m}^2$ ). ....	78
Figure 3.11: Longitude (in $^\circ\text{E}$ )-altitude (in hPa) cross-sections of (top panel) BC and (bottom panel) OC annual mass concentration ( $\mu\text{g}/\text{m}^3$ ) over the IGP (a, b, e, f) and PI (c, d, g, h) for the default and augmented model. ....	80
Figure 3.12: Seasonal variation of vertically distributed mass concentration ( $\mu\text{g}/\text{m}^3$ ) of BC over the highly polluted Indo-Gangetic Basin. ....	81
Figure 3.13: Seasonal variation of vertically distributed mass concentration ( $\mu\text{g}/\text{m}^3$ ) of OC over the highly polluted Indo-Gangetic Basin. ....	82
Figure 3.14: Spatial distribution of (a) MISR small mode AOD ('white' colour implies 'no data'), (b) AAOD simulated by default_sc, and (c) percentage increase in AAOD simulated by the augmented model w.r.t default_sc for 2010. ....	83

Figure 3.15: Seasonal variation of anthropogenic aod simulated by default and augmented model set-up.....	84
Figure 3.16: Annual variation of SW radiative forcing ( $W/m^2$ ) at TOA (left column), at the surface (middle column), and the resultant atmospheric heating ( $W/m^2$ ) (right column) for the augmented set-up. ....	85
Figure 3.17: Evaluation between model-derived surface downward shortwave flux and CERES surface shortwave flux ( $W/m^2$ ) for all-sky conditions for 2010. The black line represents the 1:1 line, and the solid red line is the curve fitting line along with red dotted predicted bounds. ....	86
Figure 3.18: Evaluation between model-derived surface downward shortwave flux and CERES surface shortwave flux ( $W/m^2$ ) for all-sky conditions for 2010. The black line represents the 1:1 line, and the solid red line is the curve fitting line along with red dotted predicted bounds. ....	86
Figure 4.1: Annual climatological distribution of the 10-year regional emissions ( $kg/m^2/s$ ) for the period 2006-2015. ....	92
Figure 4.2: 10-year climatology of the seasonal distribution of BC surface concentration ( $\mu g/m^3$ ) and corresponding changes in surface concentration ( $\mu g/m^3$ ) due to aerosol feedback effect. ....	95
Figure 4.3: 10-year climatology of the seasonal distribution of OC surface concentration ( $\mu g/m^3$ ) and corresponding changes in surface concentration ( $\mu g/m^3$ ) due to aerosol feedback effect. ....	96

Figure 4.4: 10-year climatology of the seasonal distribution of sulphate surface concentration ( $\mu\text{g}/\text{m}^3$ ) and corresponding changes in surface concentration ( $\mu\text{g}/\text{m}^3$ ) due to aerosol feedback effect. ....	97
Figure 4.5: 10-year climatology of the seasonal distribution of BC columnar burden ( $\text{mg}/\text{m}^2$ ) and corresponding changes in columnar burden ( $\text{mg}/\text{m}^2$ ) due to aerosol feedback effect. ....	98
Figure 4.7: 10-year climatology of the seasonal distribution of sulphate columnar burden ( $\text{mg}/\text{m}^2$ ) and corresponding changes in columnar burden ( $\text{mg}/\text{m}^2$ ) due to aerosol feedback effect. ....	100
Figure 4.8: 10-year climatology of the seasonal variation of ageing timescale anomaly (in hrs) for the ANTHRO experiment w.r.t the default 27.6 hrs (i.e. 1.15 day (Cooke et al., 1999)) for the period 2006-2015. ....	102
Figure 4.9: 10-year climatology of the seasonal distribution of difference (in hours) in ageing timescale between ANTHRO and CARB experiments. The difference has been calculated by subtracting CARB from ANTHRO. ....	102
Figure 4.10: Seasonal distribution of 10-year climatological ANTHRO experiment for – (a) anthropogenic AOD (1st row), (b) shortwave radiative forcing ( $\text{W}/\text{m}^2$ ) at TOA (2nd row) and (c) shortwave radiative forcing ( $\text{W}/\text{m}^2$ ) at the surface (3rd row).....	105
Figure 4.11: Seasonal distribution of the 10-year climatological difference between ANTHRO and CARB for shortwave radiative forcing ( $\text{W}/\text{m}^2$ ) at TOA (1st and 2nd rows) and the surface (3rd and 4th rows).....	106
Figure 4.12: 10-year climatology of the seasonal distribution of atmospheric heating ( $\text{W}/\text{m}^2$ ) for the period 2006-2015. ....	107

Figure 4.13: 10-year climatology of the seasonal distribution of temperature (°C) – top panel and precipitation (mm/day) – middle panel and wind at 850hPa (m/sec) - bottom panel. ....	109
Figure 4.14: Bias calculation of 10-year meteorological data – (a) annual temperature (°C), (b) annual precipitation (mm/day), (c) JJAS precipitation (mm/day) w.r.t IMD meteorological data, significant at 95% CI.....	109
Figure 4.15: Seasonal distribution of meteorological parameters, responsible for aerosol transport and distribution due to the aerosol-radiative feedback effect. ....	110
Figure 4.16: Feedback response of meteorological parameters and removal processes during winter (Jan-Feb) in the presence of anthropogenic aerosols for the period 2006-2015. The 1st column represents meteorological parameters. The 2nd column represents dry removal and the 3 <sup>rd</sup> column represents wet removal processes for hydrophobic BC (BC_HB) and OC (OC_HB) and hydrophilic BC (BC_HL) and OC (OC_HL).....	113
Figure 4.17: Seasonal distribution of AAOD due to anthropogenic aerosols feedback response obtained by subtracting CTL from ANTHRO. ....	114
Figure 4.18: Feedback response of meteorological parameters during pre-monsoon (March-April-May) in the presence of anthropogenic aerosols for the period 2006-2015. The 1st column represents meteorological parameters. The 2nd column represents dry removal, and the 3 <sup>rd</sup> column represents wet removal processes for hydrophobic BC (BC_HB) and OC (OC_HB) and hydrophilic BC (BC_HL) and OC (OC_HL).....	116

Figure 4.19: Feedback response of meteorological parameters during monsoon (Jun-Jul-Aug-Sep) in the presence of anthropogenic aerosols for the period 2006-2015. The 1st column represents meteorological parameters. The 2nd column represents dry removal, and the 3 <sup>rd</sup> column represents wet removal processes for hydrophobic BC (BC_HB) and OC (OC_HB) and hydrophilic BC (BC_HL) and OC (OC_HL).....	118
Figure 4.20: Feedback response of meteorological parameters during post-monsoon (Oct-Nov-Dec) in the presence of anthropogenic aerosols for the period 2006-2015. The 1st column represents meteorological parameters. The 2nd column represents dry removal, and the 3 <sup>rd</sup> column represents wet removal processes for hydrophobic BC (BC_HB) and OC (OC_HB) and hydrophilic BC (BC_HL) and OC (OC_HL).....	120
Figure 5.1: Contribution by various sectors towards BC, OC and SO <sub>2</sub> emissions (kg/km <sup>2</sup> /year) for the years 2006 and 2015.....	126
Figure 5.2: Annual climatological distribution of regional emissions after removing each of the five major sectors - domestic (DOM), agricultural waste burning (AWB), energy (ENE), industries (IND) and transport (TRA).....	127
Figure 5.3: Seasonal distribution of BC surface concentration anomaly (µg/m <sup>3</sup> ) w.r.t CTL experiment, significant at 95% CI. ....	130
Figure 5.4: Seasonal distribution of OC surface concentration anomaly (µg/m <sup>3</sup> ) w.r.t CTL experiment, significant at 95% CI. ....	131
Figure 5.5: Seasonal distribution of sulphate surface concentration anomaly (µg/m <sup>3</sup> ) w.r.t CTL experiment, significant at 95% CI. ....	132

Figure 5.6: Seasonal distribution of anthropogenic aerosol number concentration anomaly ( $\text{cm}^{-3}$ ) for 5 sensitivity experiments w.r.t the control simulation. ....	134
Figure 5.7: Seasonal distribution of black carbon ageing timescale anomaly ( $\text{hr}^{-1}$ ) at the surface (i.e., 1000 hPa) for 5 sensitivity experiments w.r.t the control simulation. ....	135
Figure 5.8: Seasonal distribution of % changes in anthropogenic AOD over IGB and PI in absence of each sector (mentioned sector) for five sensitivity experiments. ....	137
Figure 5.9: Seasonal distribution of % changes in surface SWRF (top panels) and atmospheric heating (bottom panels) over IGB and PI in absence of each sector (mentioned sector) for five sensitivity experiments. ....	139

## List of tables

Table 1: List of parameterisation schemes considered for the experiments .....	37
Table 2: Detailed description of the experiments .....	64